Heliyon 10 (2024) e26441

Contents lists available at ScienceDirect

Heliyon

journal homepage: www.cell.com/heliyon

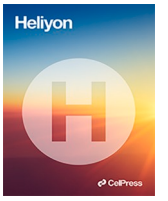

Research article

Molecular dynamics simulation of surfactant reducing MMP between CH_4 and n-decane

Zhenzhen Dong [a], Shihao Qian [a], Weirong Li [a,*], Xinle Ma [a], Tong Hou [a], Tianyang Zhang [a], Zhanrong Yang [a], Keze Lin [b], Hongliang Yi [c]

[a] Xi'an Shiyou University, Xi'an, 710065, China
[b] China University of Petroleum (Beijing), Beijing, 102249, China
[c] Liaohe Oilfield of China National Petroleum Corp, Panjin, 124000, China

ARTICLE INFO

Keywords:
Molecular dynamics simulation
Surfactants
Density profile
Diffusion properties
Intermolecular forces

ABSTRACT

Reinjecting produced methane offers cost-efficiency and environmental benefits for enhances oil recovery. High minimum miscibility pressure (MMP) in methane-oil systems poses a challenge. To overcome this, researchers are increasingly focusing on using surfactants to reduce MMP, thus enhancing the effectiveness of methane injections for oil recovery. This study investigated the impact of pressure and temperature on the equilibrium interfacial tension of the CH4+n-decane system using molecular dynamics simulations and the vanishing interfacial tension technique. The primary goal was to assess the potential of surfactants in lowering MMP. Among four tested surfactants, ME-6 exhibited the most promise by reducing MMP by 14.10% at 373 K. Key findings include that the addition of ME-6 enriching CH4 at the interface, enhancing its solubility in n-decane, improving n-decane diffusion capacity, CH4 weakens n-decane interactions and strengthens its own interaction with n-decane. As the difference in interactions of n-decane with ME-6's ends decreases, the system trends towards a mixed phase. This research sets the stage for broader applications of mixed-phase methane injection in reservoirs, with the potential for reduced gas flaring and environmental benefits.

1. Introduction

Petroleum fuels continue to serve as essential resources across various industrial sectors and remain pivotal to global energy demands [1,2]. In the current stage, after primary and secondary oil recovery, only one-third of the original oil in place (OOIP) has been extracted from oil fields, leaving 70% of OOIP still within reservoirs [3,4]. Furthermore, the challenges associated with petroleum exploration and development are escalating. Particularly, low-permeability reservoirs pose unique difficulties due to their naturally low productivity, unfavorable reservoir properties, low permeability, and challenging development processes. Consequently, gas injection enhanced oil recovery (EOR) has become the most extensively utilized method for extracting light and intermediate crude oil reservoirs, potentially elevating oil recovery rates by 10%–25% [5–7]. Among the injected gas agent, CO_2 has demonstrated the most effective oil-enhancing capabilities. However, practical oilfield conditions often present challenges such as insufficient gas sources,

* Corresponding author.
E-mail addresses: dongzz@xsyu.edu.cn (Z. Dong), LTXH990111@163.com (S. Qian), weirong.li@xsyu.edu.cn (W. Li), maxinle55@126.com (X. Ma), ht0123tong@163.com (T. Hou), zty16223334@gmail.com (T. Zhang), yzr827667468@163.com (Z. Yang), keze.lin@hotmail.com (K. Lin), yihongliang@petrochina.com.cn (H. Yi).

https://doi.org/10.1016/j.heliyon.2024.e26441
Received 10 October 2023; Received in revised form 12 February 2024; Accepted 13 February 2024
Available online 21 February 2024

high costs, and susceptibility to corrosion [8]. In contrast, using hydrocarbon gases as injection media can circumvent these drawbacks and remain unaffected by low reservoir permeability and formation water salinity [9]. For hydrocarbon gases, utilizing naturally produced gas as an injection medium not only mitigates the environmental impact of gas combustion but also supports sustainable development. If further achieving phase mixing with crude oil, the detrimental influence of interfacial tension (IFT) can be eliminated, optimizing the displacement of remaining oil within reservoirs, and thereby enhancing crude oil recovery rates.

However, for certain high-temperature reservoirs and shallow oil reservoirs, reaching the minimum miscibility pressure (MMP) between the gas and oil phases can sometimes lead to pressures exceeding the reservoir fracture pressure. Consequently, achieving phase mixing becomes challenging for such reservoirs [10]. Furthermore, the majority of miscible hydrocarbon gas injection methods are implemented within particular reservoir parameters. These parameters encompass reservoir temperatures (308 K–344 K), reservoir depths (128m–2045 m), and light crude oil (34–44 API) [11]. In such scenarios, the introduction of surfactants into the hydrocarbon-oil system can serve to reduce interfacial tension (IFT), consequently lowering the MMP between gas and oil. The change in the system's behavior, as it shifts from immiscible to partially miscible or nearly miscible injection conditions, widens the scope of applicability for miscible hydrocarbon gas injection techniques across various types of reservoirs. Hence, the reduction of MMP through the addition of surfactants to the gas-liquid biphasic system holds significant importance. This approach has the potential to enhance crude oil recovery and is crucial for expanding the scope of miscible hydrocarbon gas injection techniques to various reservoir types.

Because of its enhanced solvency and the quadrupole-quadrupole interactions occurring between carbon dioxide molecules, as opposed to the dipole interactions between methane molecules, carbon dioxide can achieve phase mixing at lower pressure [12]. This is primarily due to the shorter operating distances involved in CO_2 interactions. In contrast, the MMP between natural gas (CH_4) and crude oil is considerably higher. In the study of Hawthorne et al. [13], a comparison was made between the minimum miscibility pressures (MMP) of CH_4+oil systems and CO_2+oil systems, utilizing various crude oil compositions. The results indicated that the MMP of CH_4 is 2–3 times greater than that of CO_2. Dong et al. [14] conducted to study on the interfacial tension (IFT) of CH_4+n-decane systems and CH_4+CO_2+n-decane systems by molecular dynamics simulations. Their research indicated that the interaction between n-decane and CO_2 is notably stronger than that between n-decane and CH_4. The disparity in intermolecular forces between the two phases gives rise to interfacial tension. Crude oil molecules possess higher intermolecular forces due to the presence of permanent dipole forces and hydrogen bonding, while CH_4 molecules exhibit weaker van der Waals forces [15]. As a result, there exists a significant difference in the interaction forces between CH_4 and crude oil molecules, leading to higher interfacial tension. When there is a substantial difference in molecular forces between two substances, their interfacial tension increases, subsequently resulting in higher MMP. However, the elevated MMP levels pose challenges in achieving phase mixing between gas and liquid phases under in-situ reservoir conditions, leading to higher interfacial tension and increased residual oil saturation. Consequently, research on reducing the MMP of the CH_4-oil system is limited and inherently more challenging.

Many researchers have investigated the reduction of the MMP of the CO_2-oil system by surfactants. Guo et al. [16] synthesized a surfactant known as CAE and investigated its effect on reducing MMP through capillary tube experiments conducted at a constant temperature of 358 K while varying the pressure from 18 to 30 MPa. Their findings revealed that the addition of 0.2 wt% CAE before gas injection resulted in a 6.1 MPa reduction in MMP (a 22% decrease). Luo et al. [15] employed the Vanishing Interfacial Tension (VIT) technique was utilized to explore how nonionic surfactants impact the reduction of IFT and MMP within the CO_2-oil system. Their study demonstrated that the incorporation of 0.6 wt% propoxylated surfactant into CO_2 could lower MMP from 19.1 MPa to 13.8 MPa, representing a 27.75% reduction. Zhang et al. [17] employed ethanol as a co-solvent and utilized the VIT technique to study the effects of four distinct surfactants (2 EH-PO5-EO9, AOT, NP-9, TXIB) on reducing IFT and MMP in the CO_2-oil system. Their research indicated that in synergy with ethanol, AOT and TXIB surfactants exhibited more pronounced MMP reduction effects, achieving reductions of 7.02% and 11.85%, respectively. The above results collectively highlight that the addition of surfactants can lead to varying degrees of MMP reduction in the CO_2-oil system. Reducing the MMP in the methane and crude oil system, Mohamed Almobarak et al. [18] investigated the reduction of MMP using chemical agents in the CH_4-oil system, aiming to facilitate the injection of miscible hydrocarbon gas into high-temperature reservoirs through the use of chemical agents. They tested four different chemical additives (SOLOTERRA ME-1, SOLOTERRA ME-6, ISOFOL 16, and MARLIPAL O13) to assess their impact on lowering the Minimum Miscible Pressure. Their findings indicated that at 373 K, the utilization of a 5 wt% surfactant-based chemical, specifically SOLOTERRA ME-6, demonstrated the potential to reduce MMP by approximately 9%. Subsequently, building upon the previous study, Mohamed Almobarak et al. [19] introduced 20 mol% CO_2 into the system, resulting in a 13% reduction in MMP.

Based on the comprehensive study, it's clear that the MMP in the natural gas/CH_4-oil system is notably higher than in the CO_2-oil system. Furthermore, when compared to CH_4, adding surfactants to lower MMP in the CO_2-oil system has a more significant impact. In certain reservoirs, the pressure needed to reach the minimum MMP between gas and oil phases may exceed the formation's fracturing pressure. Therefore, there is an urgent need to explore feasible surfactants that can substantially decrease the MMP in the natural gas-oil system, thus expanding the applicability of miscible natural gas injection techniques to a wider range of potential reservoirs. Natural gas is usually a blend of different hydrocarbon gases, and the inclusion of ethane or propane tends to decrease the MMP between gas and liquid phase. Additionally, crude oil is a complex mixture with diverse components and varying proportions [13,20]. Hence, a strategy involving the use of pure CH_4 as a substitute for natural gas is viable, followed by the establishment of a CH_4-*n*-decane system molecular dynamics model. In contrast to experimental studies, molecular simulation methods offer advantages such as lower costs and fewer limitations, enabling the direct provision of microscopic insights into interfacial phenomena.

This study aims to explore the effectiveness of various surfactants in reducing the interfacial tension (IFT) between gas and liquid phases within the methane-*n*-decane system. This reduction in IFT is intended to facilitate the achievement of a miscible gas-liquid phase and, consequently, decrease the system's Minimum Miscibility Pressure (MMP). Through molecular simulations, this

research aims to uncover the underlying microscopic mechanisms behind the reduction of MMP. Section 2 introduces the molecular models established in this study, as well as the setup of the force field and parameters. In Section 3, a comparison and explanation of interfacial properties and MMP among four distinct surfactants are presented to identify the most effective one. In Section 4, an analysis of the density profile, diffusion properties, and intermolecular forces of the chosen surfactant at different pressures and temperatures is conducted to elucidate the microscale mechanisms through which the surfactant reduces MMP. Section 5 provides the concluding remarks for this study.

2. Model and simulation method

2.1. Model building

The molecular dynamics simulations in this study were conducted using the open-source software LAMMPS [21], employing different models to represent the molecules involved.

The n-decane molecule was modeled using the NERD model [22], where individual atoms were used to represent CH_3 and CH_2 groups. This model yielded gas-liquid equilibrium curves that closely matched experimental data.

CH_4 molecules were modeled using the TraPPE-UA model [23], which utilizes a single atom to represent CH_4.

Small-molecule compounds typically consist of fewer atoms, with weaker bonds and relatively smaller intermolecular forces. Such compounds often possess multiple functional groups, such as hydroxyl, acyl, amino, carbonyl, etc. These functional groups can introduce a degree of polarity to the compound, facilitating both polar and non-polar interactions during gas dissolution, thereby enhancing the gas solubility. In light of this, this study chose four chemicals to decrease the IFT in the CH_4-*n*-decane system. These include two non-ionic alkoxylate surfactants (SOLOTERRA ME-1 and ME-6) and two lipophilic alcohols (Fatty alcohol polyoxypropylene ether (SPO_5), and 2-Butoxy ethanol). The molecular structures of these selected surfactants are schematically shown in Fig. 1(a–d). The OPLS-UA model [24] was employed for all four chemical compounds, using individual atoms to represent CH_3 and CH_2 groups in both alkanes and ethers.

The periodic boundary molecular models established in this study consist of a gas-liquid system composed of a central liquid alkane

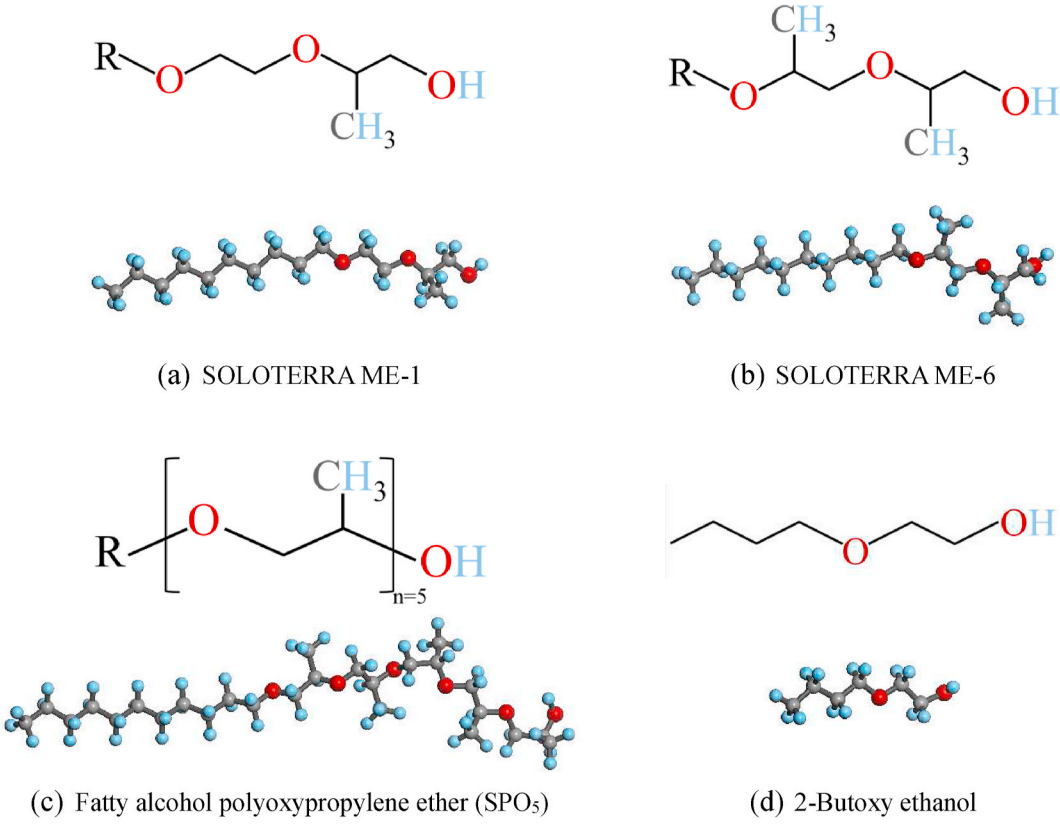

Fig. 1. Schematic molecular structures of surfactants.
represents C atoms, represents H atoms, represents O atoms.

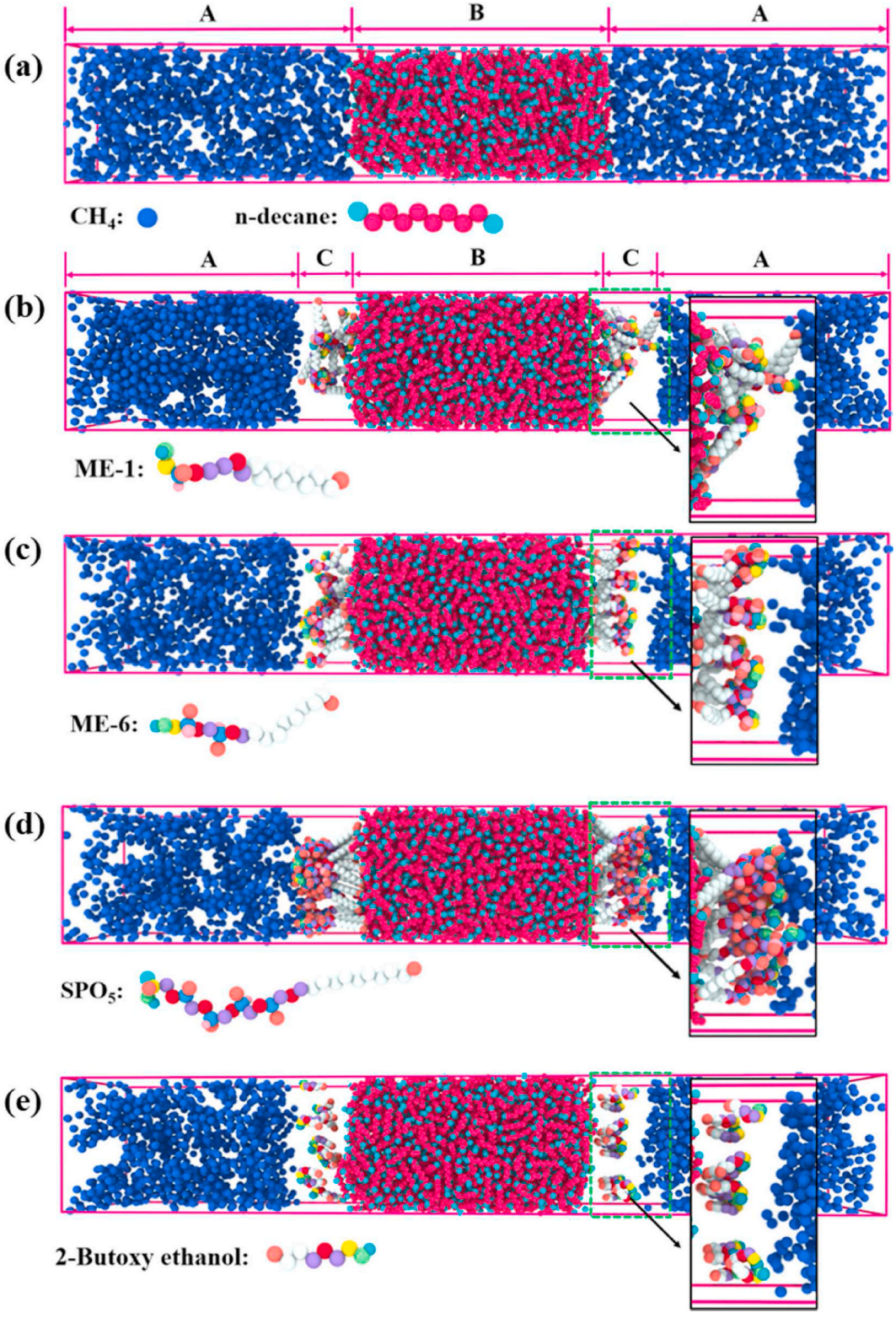

Fig. 2. Molecular Dynamics Model Diagrams: (a) CH_4+n-decane system model, (b) CH_4+SOLOTERRA ME-1+n-decane system model, (c) CH_4+SOLOTERRA ME-6+n-decane system model, (d) CH_4+SPO_5+n-decane system model, (e) CH_4+2-Butoxy ethanol + n-decane system model.

phase flanked by gas phases on both sides. An equal number of surfactant molecules are added at the gas-liquid interface on both sides. The simulation cell dimensions are 50 Å × 50 Å × 300 Å. The basic system models established include a binary system of CH_4+n-decane, as well as a ternary system of CH_4+surfactant + n-decane, as shown in Fig. 2(a–e). In this figure, region A represents methane, region B represents n-decane, and region C represents the surfactant. The system's pressure is regulated by varying the amount of CH_4 molecules added. The model contains over 10,000 atoms, with a constant number of 800 n-decane molecules (consisting of 8000 atoms) and a base number of 30 surfactant molecules (15 in each left and right region). The remaining molecules are CH_4. The visualization of the system is created using the OVITO software [25].

In this study, to keep a consistent temperature during the entire MD simulation, the Nosé-Hoover thermostat was employed for temperature control [26,27]. Utilizing the particle-particle-particle-mesh (PPPM) summation method, the long-range electrostatic interactions were computed with a precision of 1.0×10^{-4} [28]. To reduce truncation and system size influences in interface property calculations, a unit cell of 5×5 nm^2 was selected parallel to the interface direction and a cutoff radius of 2 nm (Approx.6σ) was set for non-bonded interactions [29–31]. The simulation time step was set to 1 fs. The entire simulation duration included a 500 ps equilibration period, a 10 ns relaxation period, and a 20 ns production period. Statistical analysis was performed every 10 ps to calculate the system's IFT.

The formula for calculating IFT is given by equation (1) [32–34].

$$\gamma = \frac{1}{2}\int_0^{L_z} (P_N(z) - P_T(z))\mathrm{d}z = \frac{1}{2}\left[P_{zz} - \frac{P_{xx} + P_{yy}}{2}\right]L_z \tag{1}$$

where γ represents the IFT, $P_N(z)$ and $P_T(z)$ denote the normal and tangential pressures, $P_{\alpha\alpha}$ $(\alpha = x, y, z)$ signifies the diagonal elements of the pressure tensor, and L_z represents the length of the simulated system along the z-direction.

Atomic diffusion behavior is characterized by the time-dependent change in mean square displacement (MSD) [35].There is the MSD calculation formula (2):

$$\mathrm{MSD(t)} = \langle |r_i(t) - r_i(0)|^2 \rangle \tag{2}$$

Here, $r_i(0)$ denotes the initial position of atom *i*, and $r_i(t)$ denotes the position of atom *i* at time t.

To examine fluid molecule aggregation and analyze fluid microstructure, use the radial distribution function. This function reflects the likelihood of locating another atom at a specific distance from a given atom and can be seen as the ratio of local density to the system's overall density within a defined region [36]. The expression is given by the following equation (3):

$$g(r) = \frac{dN}{\rho 4\pi r^2 dr} \tag{3}$$

In which, *N* represents the number of atoms, *r* stands for the distance between two atoms, and ρ denotes the system density.

2.2. Force field and parameters

One of the purposes of conducting molecular dynamics simulations is to obtain the potential energy functions for different systems. The potential energy function that describes the interatomic interactions within a system is referred to as a force field. In general, a molecular force field can be considered as a sum of various potentials, primarily including molecular interaction potentials such as bond stretching, bond angle bending, and dihedral angle torsional potentials, along with van der Waals and Coulombic electrostatic potentials, all of which are detailed in equations (4)–(11).

$$U_{total} = U_{stretch} + U_{bend} + U_{torsion} + U_{coul} + U_{vdw} \tag{4}$$

In this study, bond stretching and bond angle bending potentials are represented using harmonic terms, while the dihedral angle torsional potential employs the OPLS (Optimized Potentials for Liquid Simulations) functional form. The bond stretching potential is defined as follows:

$$U_{stretch} = K_r(r - r_0)^2 \tag{5}$$

The bond angle bending potential is defined as follows:

$$U_{bend} = K_\theta(\theta - \theta_0)^2 \tag{6}$$

The torsional potential energy is expressed by the following formula:

$$U_{torsion} = V_0 + V_1(1 + \cos\varphi) + V_2[1 - \cos(2\varphi)] + V_3[1 - \cos(3\varphi)] \tag{7}$$

where *r*, r_0 denote the equilibrium bond length and known bond length, θ_0, θ stand for the known bond angle and equilibrium bond angle, K_θ, K_r, and V_n $(n = 0, 1, 2, 3)$ represent the bond angle bending potential, constants for bond stretch potential, and dihedral angle torsion potential.

The Coulomb potential energy can be derived from Coulomb's law, as shown in the following formula:

$$U_{coul} = \frac{q_i q_j}{4\pi\varepsilon_0 r_{ij}} \tag{8}$$

where q_i (q_j) represents the charge of atom i (j), ε_0 is the dielectric constant, and r_{ij} is the distance between atom i and atom j.

The van der Waals potential energy can be obtained from the 12-6 Lennard-Jones potential function, as shown in the following formula:

$$U_{vdw} = 4\varepsilon_{ij}\left[\left(\frac{\sigma_{ij}}{r_{ij}}\right)^{12} - \left(\frac{\sigma_{ij}}{r_{ij}}\right)^{6}\right] \tag{9}$$

where, the short-range interactions are characterized by ε_{ij}, representing the well depth, and σ_{ij}, which denotes the core diameter of the Lennard-Jones potential.

Mixing rules are employed to calculate the Lennard-Jones (L-J) parameters for various pairs of atoms, with the commonly used Lorentz-Berthelot mixing rules [37], as shown in the following formula:

$$\varepsilon_{ij} = \sqrt{\varepsilon_i \varepsilon_j} \tag{10}$$

$$\sigma_{ij} = \frac{\sigma_i + \sigma_j}{2} \tag{11}$$

Table 1 presents the parameters of each force field utilized in this study.

Table 1
Force field parameters for each molecule.

Molecular	Atom	(nm)	(KJ·mol^{-1})	(e)	Model
n-decane	CH_3	0.3910	0.8647	0	NERD [22]
	CH_2	0.3930	0.3808	0	
CH_4	CH_4	0.3730	1.2300	0	TraPPE-UA [23]
SOLOTERRA ME-6	CH_3 (in C–C bond)	0.3910	0.6694	0	OPLS-UA [24]
	CH_2 (in C–C bond)	0.3905	0.4937	0	
	CH_2 (in O–C bond)	0.3800	0.4937	0.250	
	CH_2 (in C–OH bond)	0.3905	0.4937	0.265	
	C (in O–C bond)	0.3500	0.2761	0.170	
	O (in O–C bond)	0.3000	0.7112	−0.500	
	O (in O–H bond)	0.3120	0.7112	−0.683	
	H (in C–C–H bond)	0.2500	0.1255	0.030	
	H (in O–H bond)	0	0	0.418	
SOLOTERRA ME-1	CH_3 (in C–C bond)	0.3910	0.6694	0	
	CH_2 (in C–C bond)	0.3905	0.4937	0	
	CH_2 (in O–C bond)	0.3800	0.4937	0.250	
	CH_2 (in C–OH bond)	0.3905	0.4937	0.265	
	C (in O–C bond)	0.3500	0.2761	0.170	
	O (in O–C bond)	0.3000	0.7112	−0.500	
	O (in O–H bond)	0.3120	0.7112	−0.683	
	H (in C–C–H bond)	0.2500	0.1255	0.030	
	H (in O–H bond)	0	0	0.418	
Fatty alcohol polyoxypropylene ether （SPO_5）	CH_3 (in C–C bond)	0.3910	0.6694	0	
	CH_2 (in C–C bond)	0.3905	0.4937	0	
	CH_2 (in O–C bond)	0.3800	0.4937	0.250	
	C (in C–OH bond)	0.3500	0.2761	0.205	
	C (in O–C bond)	0.3500	0.2761	0.170	
	O (in O–C bond)	0.3000	0.7112	−0.500	
	O (in O–H bond)	0.3120	0.7112	−0.683	
	H (in C–C–H bond)	0.2500	0.1255	0.030	
	H (in O–C–H bond)	0.2500	0.1255	0.040	
	H (in O–H bond)	0	0	0.418	
2-Butoxy ethanol	CH_3 (in C–C bond)	0.3910	0.6694	0	
	CH_2 (in C–C bond)	0.3905	0.4937	0	
	CH_2 (in O–C bond)	0.3800	0.4937	0.250	
	CH_2 (in C–OH bond)	0.3905	0.4937	0.265	
	O (in O–H bond)	0.3120	0.7112	−0.683	
	H (in O–H bond)	0	0	0.418	

3. Surfactants preferred

3.1. Force field verification

For assessing the Minimum Miscibility Pressure (MMP) in the CH_4-*n*-decane system, this study utilized the well-established Vanishing Interfacial Tension (VIT) method, which is commonly employed for MMP determination [38–40]. In the VIT method, a constant temperature is maintained while measuring the equilibrium Interfacial Tension (IFT) between the gas and crude oil at different pressure levels. For estimating bulk properties, the study uses the Volume Translated Predictive Peng-Robinson 1978 (VT-PPR78) [41, 42] equation of state (EoS) in conjunction with standard van der Waals one-fluid mixing rules and a linear mixing rule for volume correction [43]. Supplementing the simulated data and calculating interfacial properties, the study employs theoretical modeling that combines the VT-PPR78 equation of state (EoS) with density gradient theory (DGT). The Minimum Miscibility Pressure (MMP), denoting the minimum pressure needed to attain phase miscibility, is represented by the point where the estimated curve intersects with the pressure axis [44]. The Vapor-Liquid Equilibrium Interfacial Tension (VIT) is rooted in the concept that miscibility is achieved when the interfacial tension (IFT) between two distinct phases is eradicated.

In our previous work [14], Molecular Dynamics (MD) simulations were utilized to investigate the IFT of the CH_4+n-decane mixture system at various temperatures. The MD simulation results, as depicted in Fig. 3, closely matched the experimental data presented by Pereira [45] and the MD simulation outcomes by Choudhary et al. [43]. Therefore, utilizing the same MD model and molecular force field, we conducted simulations to estimate the IFT at 373.0 K. Additionally, estimations obtained through the Diffuse Gradient Theory (DGT) and the Volume-Translated Peng-Robinson 1978 Equation of State (VTPPR78 EoS) are depicted as lines in the graph. From Fig. 3, it can be observed that at a temperature of 373.0 K, the Interfacial Tension (IFT) measured using MD aligns with the results obtained from previous studies. Consistent with findings in the literature, the IFT in the CH_4+n-decane system diminishes with an increase in system pressure [41,43]. Under low pressures, increasing temperature results in a more significant decrease in the system's IFT, whereas at high pressures, the IFT remains stable. This study utilized a molecular force field that is suitable for the investigated system, along with the specified parameters and settings.

3.2. Density profile

Fig. 4 depicts the density distribution of n-decane and methane along the vertical interface direction in the n-decane + methane system at 373.0 K and 11.09 MPa after reaching equilibrium with the addition of different surfactants. The dashed lines represent the density distribution without surfactants, while the solid lines represent the density distribution with surfactants. Figure 4a shows the density distribution of n-decane, Fig. 4(b) shows the density distribution of CH_4. The graph clearly illustrates that the introduction of surfactants causes a reduction in the density of n-decane, leading to an expansion of the volume occupied by the liquid phase. The CH_4

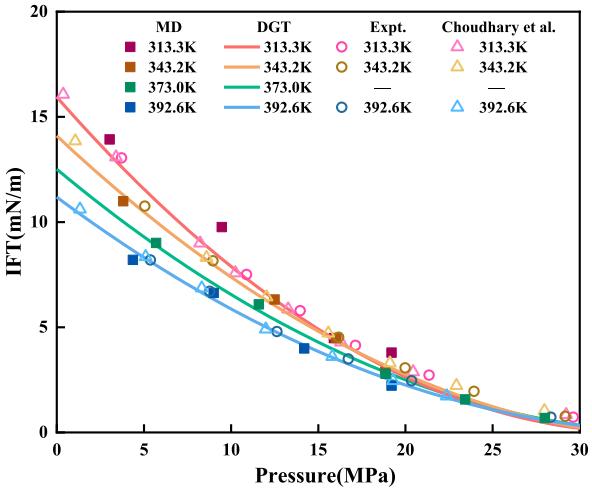

Fig. 3. Interfacial tension (IFT) of CH_4+n-decane at different temperatures.
■ represents the results from MD simulations (■ 313.3 K, ■ 343.2 K, ■ 373.0 K, ■ 392.6 K) and the estimates obtained using the DGT with VT-PPR78 EoS are shown as lines (— 313.3 K, — x 343.2 K, — 373.0 K, — 392.6 K). Experimental results by Pereira [45] are depicted as ○ (○ 313.3 K, ○ 343.2 K, ○ 392.6 K). △Displays the MD simulation results by Choudhary et al. [43] (△ 313.3 K, △ 343.2 K, △ 392.6 K).

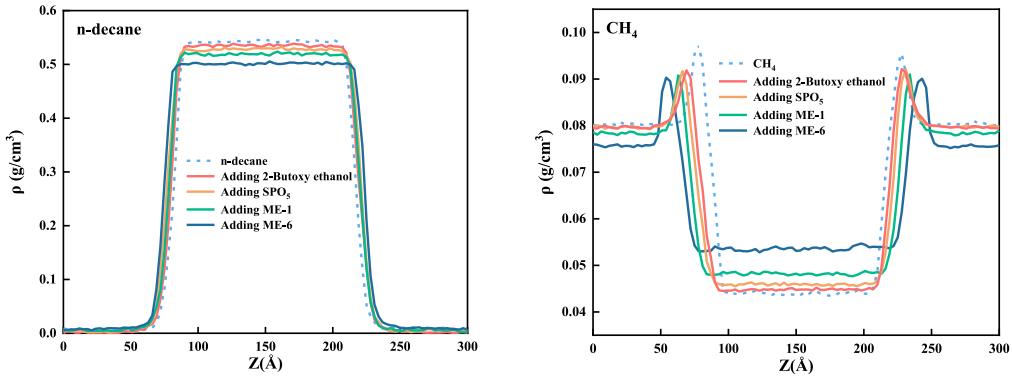

(a) The number density distribution of n-decane (b) The number density distribution of CH_4

Fig. 4. Number density distribution of CH_4/n-decane with different surfactants added (373.0 K, 11.09 MPa).

phase experiences an increase in density, resulting in a thicker phase interface. This indicates that the incorporation of surfactants facilitates better diffusion of CH_4 molecules into the n-decane phase, enhancing the degree of mixing and increasing the mixed phase volume. Notably, surfactant ME-6 demonstrates a more pronounced effect in reducing n-decane phase density and increasing CH_4 phase density.

Fig. 5(a–e) illustrates the impact of four types of surfactants (2-Butoxy ethanol, SPO_5, ME-1, and ME-6) on the phase behavior of the CH_4 + n-decane system. From the graph, it is evident that under the conditions of 373.0 K and 27.51 MPa, without the addition of surfactants, there is a distinct interface on both sides of the CH_4 + n-decane system. The CH_4 and n-decane components are separated into two distinct phases and have not reached complete mixing. Upon the addition of these four different surfactants, the volume of the mixed phase in the system increases, and the degree of mixing improves to varying extents. Particularly, with the inclusion of surfactant ME-6, the interface between CH_4 and n-decane is no longer discernible in the system, essentially achieving a fully mixed state for the CH_4 + n-decane system under the influence of ME-6.

The density distribution curves in Fig. 6(a and b) also support this observation. After the addition of surfactant ME-6, the density of the n-decane phase decreases, while the density of the CH_4 phase increases. Furthermore, both the n-decane and CH_4 phases are uniformly distributed throughout the system's container, approaching an average density. This indicates a significant increase in the degree of mixing between the n-decane and CH_4 phases, thus confirming the achievement of a mixed phase state in the system.

3.3. Diffusion properties

To examine the diffusion characteristics of n-decane and CH_4 under various surfactant conditions as well as without surfactants, the mean square displacement (MSD) of these substances was determined at 373.0 K and 22.84 MPa. As shown in Figure 7a, it is noticeable that the diffusion rate of n-decane increases to varying degrees in the presence of different surfactants. As the diffusion rate of n-decane increases, a greater number of n-decane molecules occupy the adsorption sites initially held by methane molecules. This restriction limits the free movement space of methane molecules, resulting in increased steric hindrance for CH_4 molecules. Therefore, the diffusion rate of CH_4 decreases after the addition of surfactants (as shown in Fig. 7(b)). Among these four surfactants (2-Butoxy ethanol, SPO_5, ME-1, and ME-6), surfactant ME-6 is particularly noteworthy for significantly enhancing the diffusion rate of n-decane while diminishing the diffusion rate of CH_4.

3.4. Intermolecular forces

To systematically identify the most effective surfactant on a microscopic level after adding different surfactants, the radial distribution functions (g(r)) between different molecules were investigated for various surfactant conditions (2-Butoxy ethanol, SPO_5, ME-1, and ME-6). Figure 8a presents the radial distribution function depicts the interactions among n-decane molecules, while Fig. 8 (b) illustrates the radial distribution function depicts the interactions between n-decane and methane molecules.

From Figure 8a, it can be observed that under the same conditions (373.0 K, 11.09 MPa), the peak values of g(r) for different surfactants are lower than that of the system without surfactant, indicating a reduction in the interaction force between n-decane molecules. Among these conditions, the addition of surfactant ME-6 exhibits the most significant decrease in peak value, indicating the strongest reduction in interaction force between n-decane molecules. Fig. 8(b) demonstrates that under the same conditions (373.0 K, 11.09 MPa), the peak values of g(r) with different surfactants are higher than that of the system without surfactant. This suggests that the addition of surfactants enhances the interaction forces between methane and n-decane molecules. Among these conditions, surfactant ME-6 shows the highest increase in peak value, indicating the most pronounced enhancement in the interaction force between methane and n-decane molecules.

After the introduction of surfactants, the distance between n-decane molecules increases, while the separation between methane

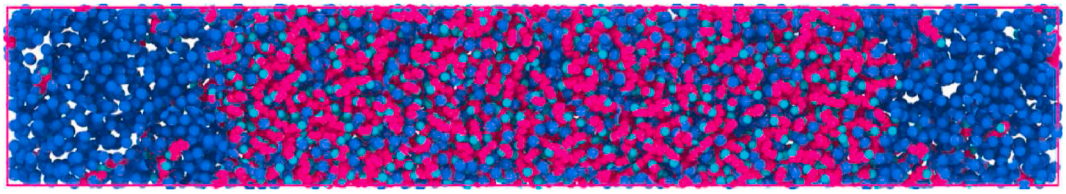

(a) No surfactant

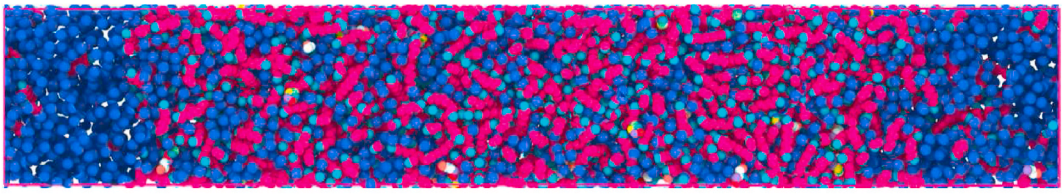

(b) Addition of 2-Butoxy ethanol

(c) Addition of SPO_5

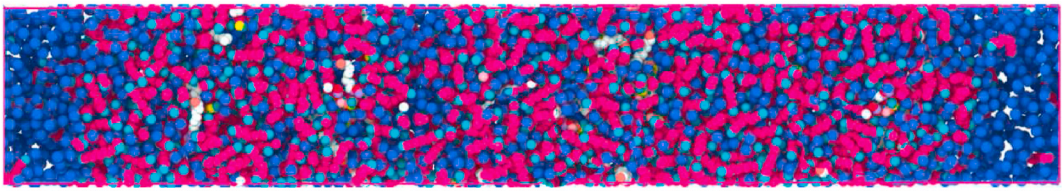

(d) Addition of ME-1

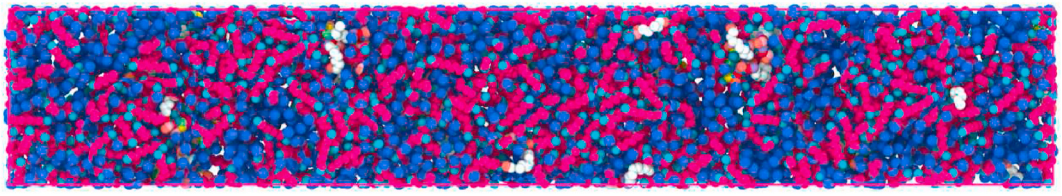

(e) Addition of ME-6

Fig. 5. Effect of Four Surfactants on the Phase Behavior of CH_4 + n-decane System at 373.0 K, 27.51 MPa.

and n-decane molecules decreases. This is attributed to the distribution of surfactants at the oil-gas interface, causing n-decane to be surrounded by methane molecules. As a result, the quantity of dissolved methane in n-decane increases, leading to improved mixing between methane and n-decane molecules, thus enhancing the phase mixing effect between them.

3.5. Interfacial tension and miscibility pressure

During the force field validation, the IFT of the CH_4 + n-decane system at 373.0 K was determined. Additionally, utilizing estimates obtained from the DGT and VTPPR78 EoS methods, the MMP for the system at that temperature was derived in the absence of surfactants. In this system, various surfactant molecules (ME-1, ME-6, SPO_5, and 2-Butoxy ethanol) were separately introduced, as depicted in Fig. 9. The IFT reduction results for the CH_4 + n-decane system with these four surfactants at 373.0 K were obtained, and the corresponding MMP values for different surfactant systems were calculated (as shown in Table 2). From the figures and tables, it can be observed that at 373.0 K, the introduction of these four surfactants into the CH_4 + n-decane system results in a decrease in the

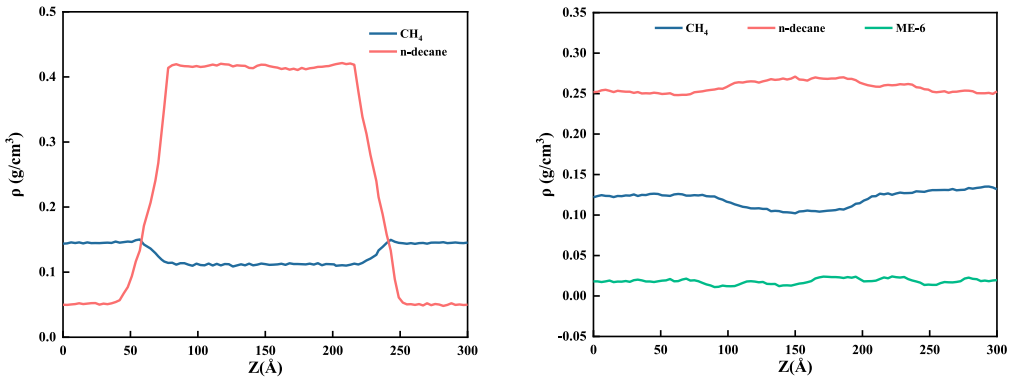

(a) Without surfactant (b) With surfactant ME-6

Fig. 6. Effect of Surfactant ME-6 on the Density Distribution Curve of CH_4 + n-decane System at 373.0 K, 27.51 MPa.

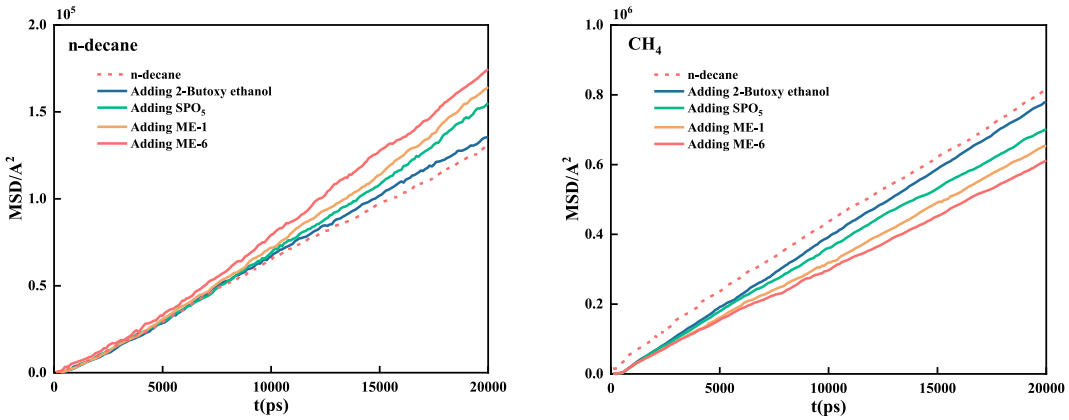

(a) MSD of n-decane (b) MSD of CH_4

Fig. 7. MSD of n-decane/CH_4 at different surfactants at 373.0 K, 22.84 MPa.

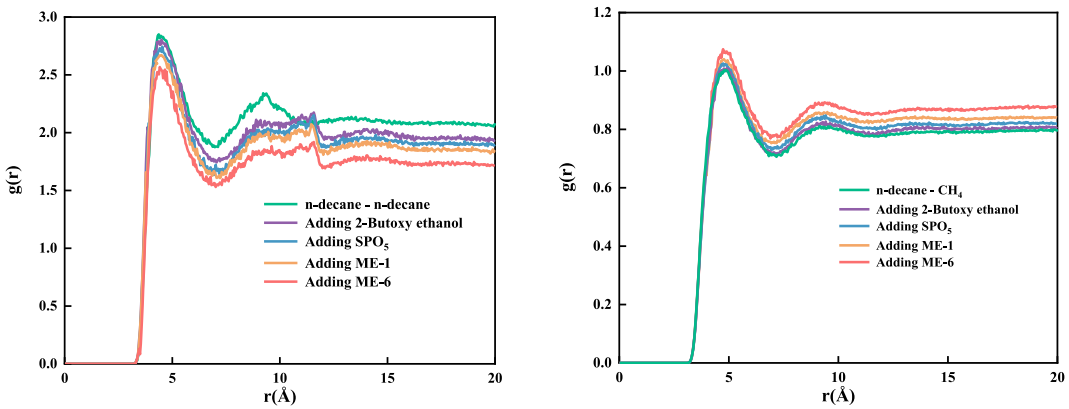

(a) N-decane-n-decane (b) n-decane-CH_4

Fig. 8. Radial distribution function of n-decane/CH_4 before and after the addition of ME-6 (373.0 K , 11.09 MPa).

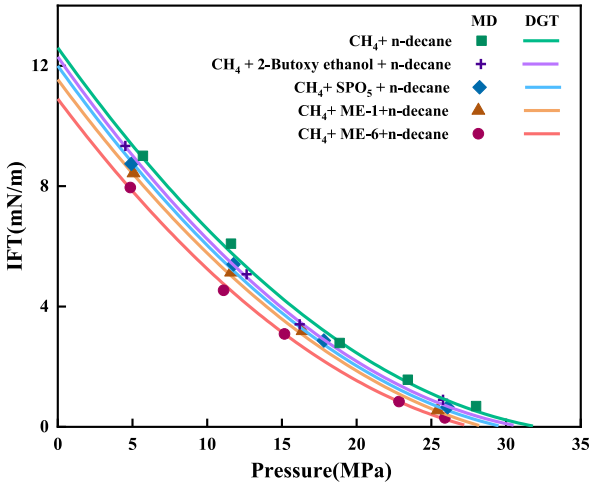

Fig. 9. Interfacial Tension (IFT) of CH_4 + Surfactant + n-decane System at 373.0 K. The symbols represent the results from the MD simulations, and the estimates obtained using the DGT with VTPPR78 EoS are depicted as lines.

Table 2
MMP of CH_4 + different surfactants + n-decane system at 373.0 K.

Chemical	MMP (MPa)	MMP reduction
Base case	32.12	–
2-Butoxy ethanol	31.12	3.08%
SPO_5	29.83	7.13%
ME-1	28.51	11.24%
ME-6	27.59	14.10%

MMP of the CH_4-*n*-decane system. The surfactants 2-Butoxy ethanol, SPO_5, ME-1, and ME-6 lead to reductions in the system's MMP by 3.08%, 7.13%, 11.24%, and 14.10%, respectively. While the effect of 2-Butoxy ethanol on reducing the system's IFT is not significant, the addition of ME-6 surfactant results in a notable decrease in the IFT of the CH_4 + n-decane system. As a result, the system's MMP is lowered from 32.12 MPa to 27.59 MPa, marking a reduction of 14.10%.

Comparing ME-1, ME-6, SPO_5, and 2-Butoxy ethanol surfactants at 373.0 K across various aspects such as Density Profiles, Diffusion Properties, Intermolecular Forces, Interfacial Tension, and Miscibility Pressure, the results indicate that ME-6 surfactant has more favorable effects. It reduces the density of the n-decane phase while increasing the density of the CH_4 phase. It effectively enhances the n-decane diffusion rate while diminishing the CH_4 diffusion rate. The addition of ME-6 surfactant diminishes intermolecular forces between n-decane molecules and significantly augments forces between CH_4 and n-decane molecules. Furthermore, ME-6 surfactant notably reduces the Interfacial Tension (IFT) of the CH_4 + n-decane system, leading to a 14.10% reduction in the system's Minimum Miscibility Pressure (MMP). In summary, ME-6 surfactant shows potential in decreasing the IFT of the gas-liquid phases in the methane-*n*-decane system, facilitating phase mixing and ultimately lowering the MMP of the system. The subsequent section will delve into an analysis of the interfacial properties of ME-6 surfactant in the CH_4 + n-decane system across different pressures and temperatures. It will also explore the microscopic mechanism behind the reduction in interfacial tension caused by ME-6 surfactant.

4. Microscopic mechanisms at different temperatures and pressures

4.1. Interfacial properties of CH_4+ME-6+n-decane system under different pressure

4.1.1. Density profile

Under different pressure conditions, Fig. 10(a–e) illustrates the equilibrium state of CH_4 + ME-6 + n-decane at 373.0 K. Initially, methane molecules congregate at the interface between the two phases. As pressure increases, the number of molecules at the interface grows, with methane molecules entering the n-decane phase. The mass density distribution curves clearly showcase the interface structure between n-alkanes and methane. Once the system attains its ultimate equilibrium at 373.0 K, Fig. 11(a and b) depicts the distribution of density along the vertical interface direction of n-decane and CH_4. Dashed lines represent density distribution in a system without surfactants, while solid lines depict density distribution in the system with the addition of ME-6 surfactant. As system pressure rises, a portion of CH_4 dissolves into the n-decane phase, leading to a reduction in n-decane density and gradual expansion of the liquid phase. Simultaneously, certain n-decane molecules evaporate into the gas phase, increasing gas phase density and causing

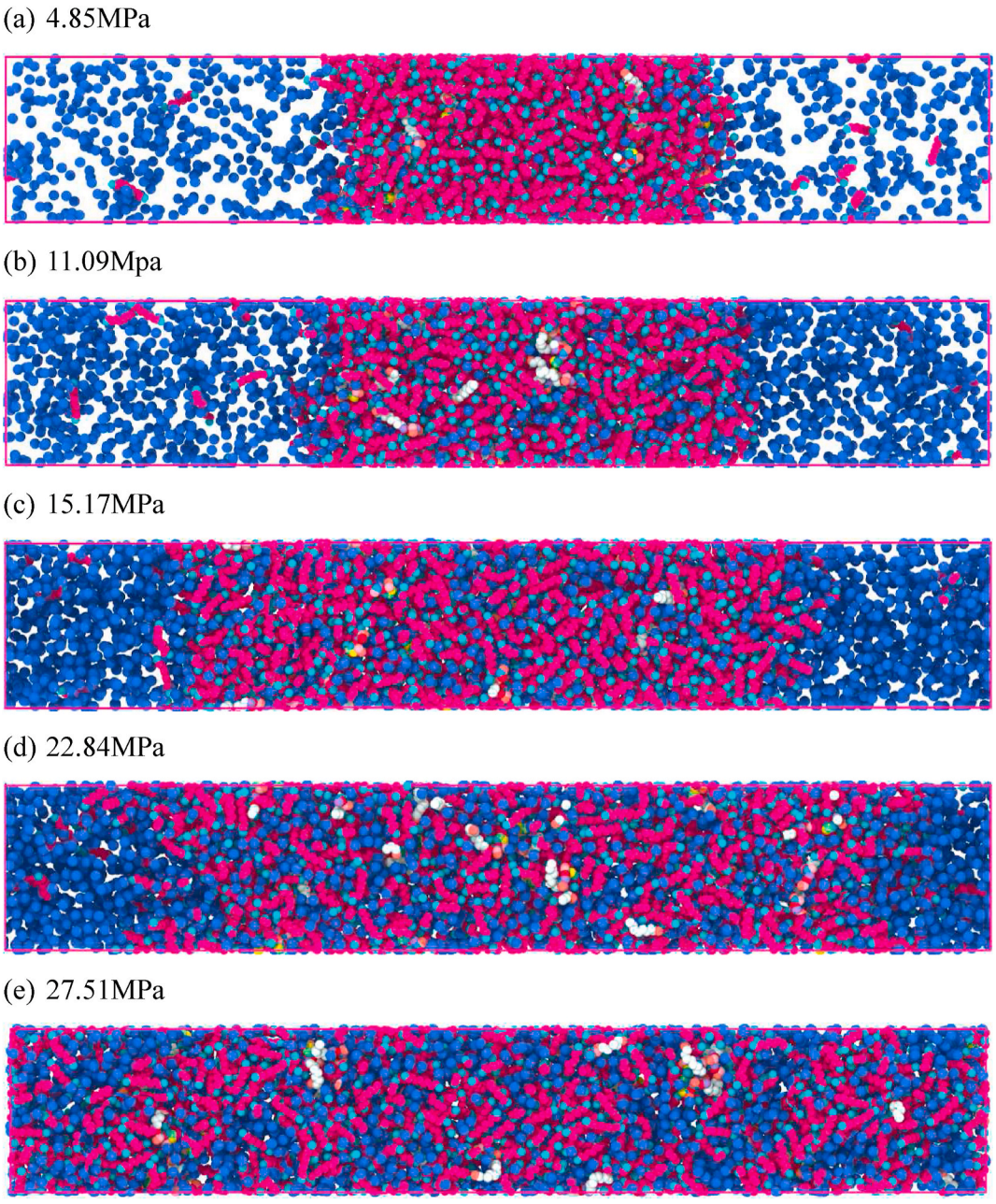

Fig. 10. Equilibrium State of the CH_4 + ME-6 + n-decane System at 373.0 K.

the phase interface to gradually thicken. Particularly in systems with added surfactants, the density of methane at the interface decreases, further enhancing the thickness of the phase interface.

4.1.2. Diffusion properties

In order to investigate the diffusion characteristics of n-decane and CH_4 with or without the addition of ME-6 surfactant, the Mean Square Displacement (MSD) of n-decane and CH_4 was calculated under different pressures. As shown in Fig. 12(a and b), it can be observed that regardless of whether ME-6 surfactant is added, the diffusion rate of n-decane increases with pressure, while the diffusion rate of CH_4 decreases with pressure. This is due to the increase in n-decane's diffusion rate as CH_4 solubility increases. Simultaneously, as pressure rises, the influence of intermolecular forces between n-decane and CH_4 becomes more pronounced, causing a higher number of n-decane molecules taking up the adsorption sites previously occupied by CH_4 molecules. Consequently, the space for CH_4 molecule free movement diminishes, leading to more collisions among CH_4 molecules in a smaller space. This increases resistance at the spatial points, ultimately resulting in a rapid decline in diffusion rate.

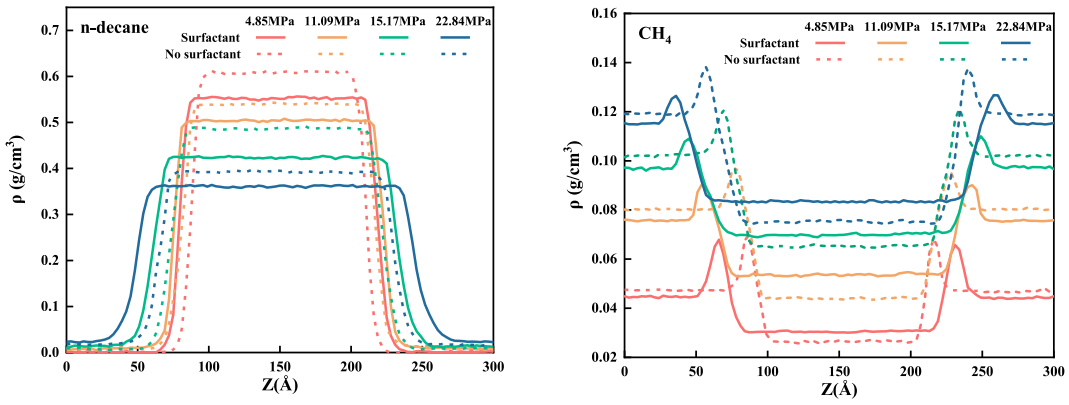

(a) Number Density Distribution of n-decane. (b) Number Density Distribution of CH_4

Fig. 11. Number density distribution of CH_4/n-decane at different pressures (373.0 K).

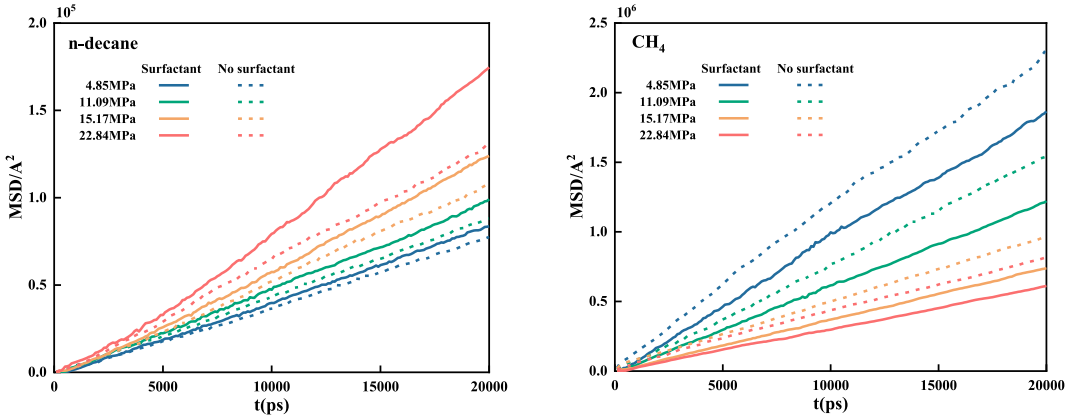

(a) MSD of n-decane (b) MSD of CH_4

Fig. 12. MSD of n-decane/CH_4 at different pressures at 373.0 K.

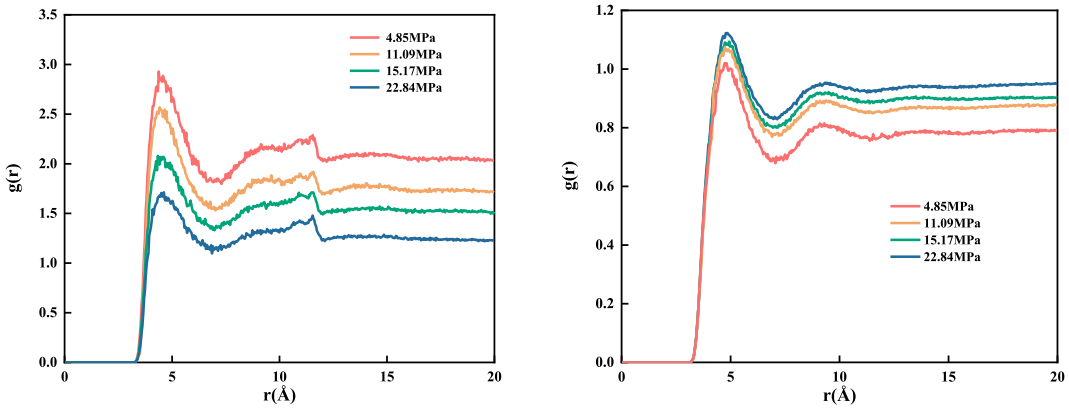

(a) n-decane-n-decane (b) n-decane-CH_4

Fig. 13. Radial distribution function of n-decane/CH_4 in the CH_4+ME-6+n-decane system at different pressures (373.0 K).

The addition of ME-6 surfactant significantly boosts the diffusion rate of n-decane, especially at high-pressure conditions where the increase in n-decane diffusion rate is more pronounced compared to cases without surfactant. Moreover, the introduction of ME-6 greatly enhances the intermolecular forces between n-decane and CH_4, leading to an increased occupation of adsorption sites by n-decane molecules, which were originally occupied by CH_4 molecules. This further diminishes the space for CH_4 molecule free movement, leading to increased resistance at spatial points. Particularly, at low-pressure conditions, the diffusion rate of CH_4 decreases faster when ME-6 surfactant is added compared to cases without surfactant.

4.1.3. Intermolecular forces

To gain further insight into the microstructural impact of adding ME-6 surfactant on the diffusion of CH_4 in relation to n-decane diffusion, the radial distribution functions (g(r)) of CH_4 and n-decane were analyzed in the CH_4 + ME-6 + n-decane system under various pressures, as depicted in Fig. 13. In Figure 13a, as the system pressure increases, the peak of g(r) for n-decane with n-decane decreases, indicating a reduction in the surrounding n-decane molecules. When combined with Fig. 13(b), the peak of g(r) for CH_4 and n-decane increases as the system pressure rises, implying an increase in the surrounding CH_4 molecules. These observations collectively suggest that with an increase in system pressure, an increasing number of CH_4 molecules are dissolved into the n-decane phase. Since CH_4 possesses a higher intrinsic diffusion coefficient compared to n-decane, this enhances the diffusion capacity of n-decane, leading to improved diffusion ability.

SOLOTERRA ME-6 is a non-ionic surfactant and a propoxylated alcohol. The SOLOTERRA ME-6 molecule consists of a hydrophobic hydrocarbon chain and a hydrophilic propoxylated group, exhibiting amphiphilic properties. Therefore, in this study, the amphiphilicity of the surfactant is thought to stem from the contrast between the oleophobic propoxylated head group and the oleophilic hydrocarbon chain of the alcohol. Upon the introduction of ME-6 surfactant into a CH_4 displacement system, surfactant molecules adhere to the interface between the gas and oil phases, facilitating the formation of a miscible region. This process takes place when the surfactant's head unit engages with CH_4 molecules, while the oleophilic tail (hydrocarbon chain) attaches to the crude oil, forming a stable molecular layer.

In this context, the oleophilic end of the surfactant interacts with the crude oil, while the oleophobic end interacts with CH_4. When the forces associated with these interactions are essentially balanced, the arrangement of molecules at the oil-gas interface is altered, reducing the repulsion between the oil and gas phases. Consequently, this lowers the interfacial tension between the two phases, facilitating miscibility. As shown in Fig. 14(a), with increasing pressure, the peak of the g(r) function between n-decane molecules and the oleophilic end of ME-6 gradually decreases, while in Fig. 14(b), the peak of the g(r) function between CH_4 and the oleophobic end of ME-6 exhibits an opposite trend. This reflects that as the disparity between the forces of interaction between n-decane molecules and the oleophilic end of ME-6, and the forces between CH_4 and the oleophobic end of ME-6 diminishes, the system approaches a mixed-phase state.

4.2. Interfacial properties of CH_4+ME-6+n-decane system at different temperatures

4.2.1. Density profile

Fig. 15(a–c) depicts the equilibrium states of CH_4+ME-6+n-decane at different temperatures under 22.84 MPa pressure. In comparison between 373.2 K and 343.2 K temperatures, at 373.2 K, the CH_4+ME-6+n-decane system exhibits a thicker phase interface, with more methane molecules entering the n-decane phase and an increased number of n-decane molecules evaporating into the gas phase. When comparing 373.2 K and 392.6 K temperatures, the differences in phase interface for the CH_4+ME-6+n-decane system at these two temperatures are relatively small. It's evident that the presence of ME-6 surfactant is more conducive to reducing the interfacial tension in the CH_4+n-decane system at higher temperatures, thereby promoting miscibility.

Fig. 16. Number density distribution of CH_4 and n-decane at the gas-liquid interface under 22.84 MPa conditions and various

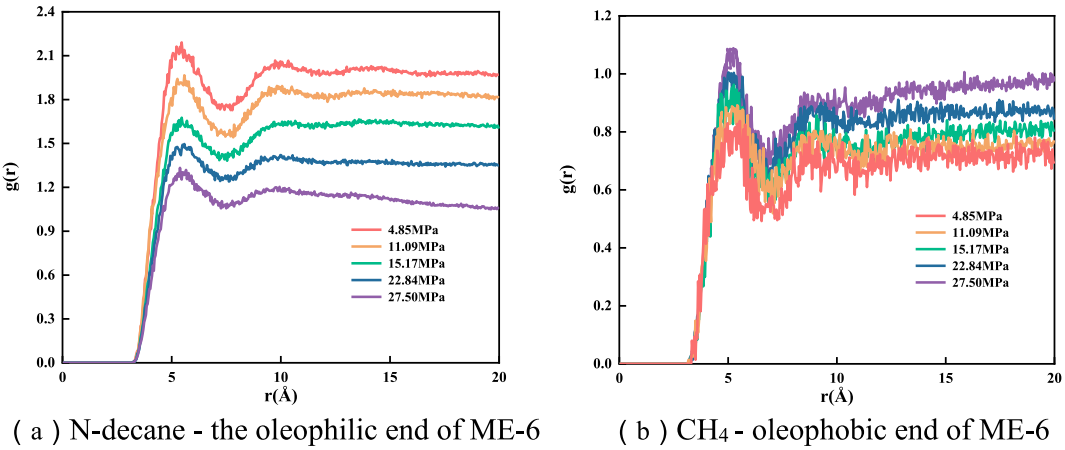

Fig. 14. Radial distribution functions between different components at various pressures (373.0 K).

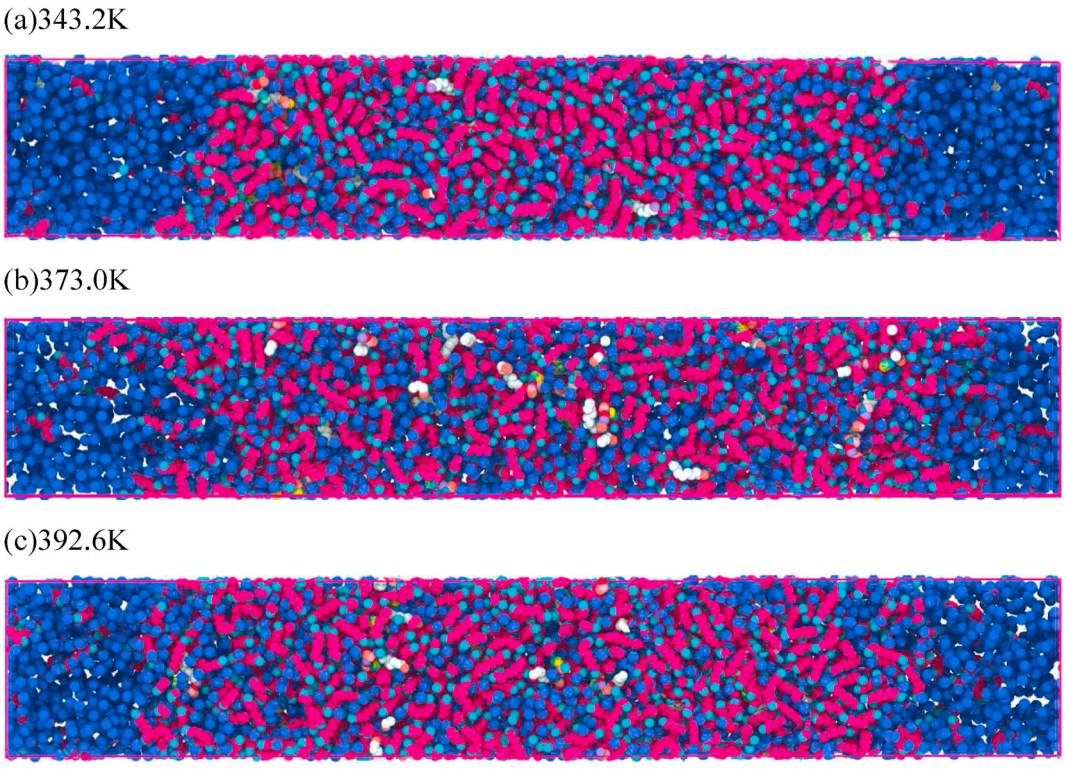

Fig. 15. Equilibrium states of the CH_4+ME-6+n-decane system at different temperatures (22.84 MPa).

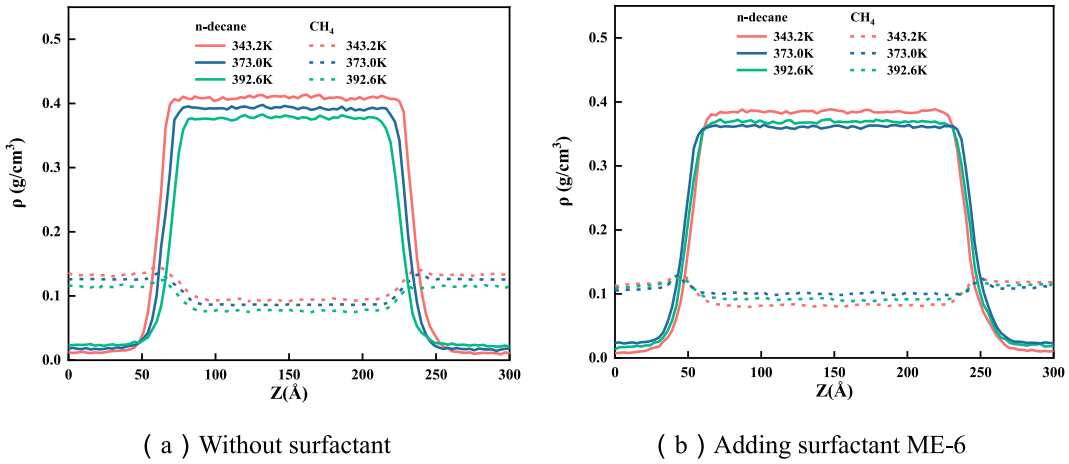

Fig. 16. Mass density distribution of CH_4/n-decane at different temperatures under 22.84 MPa.

temperatures. In Fig. 16(a), at high-pressure conditions in the CH_4+n-decane system, the number density distribution of n-decane in the liquid phase decreases slightly with increasing temperature, while the number density of CH_4 also decreases as the temperature rises. In Fig. 16(b), with the addition of the surfactant ME-6 in the CH_4+n-decane system, there is a significant increase in the mixed-phase volume and a decrease in n-decane phase density, accompanied by an increase in CH_4 phase density. Surfactant ME-6 at temperatures of 373.0 K and 392.6 K promotes the evaporation of n-decane molecules into the gas phase and the dissolution of CH_4 molecules into n-decane. Overall, the surfactant performs better in reducing n-decane phase density and increasing CH_4 phase density, resulting in a thicker mixed-phase interface and larger mixed-phase volume, especially at higher temperatures.

To further understand the trend of interfacial tension (IFT) in the system with the addition of surfactant at different temperatures, the solubility of gases in oil, i.e., the gas density in the oil phase divided by the oil density in the oil phase, was evaluated using density distributions (Fig. 16). Fig. 17 illustrates the change in CH_4 solubility in n-decane at different temperatures. From the graph, it can be

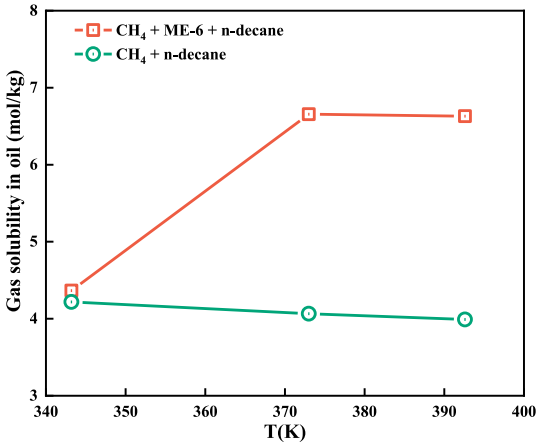

Fig. 17. Relationship between the Solubility of CH_4 in n-decane and Temperature (22.84 MPa).

observed that without the surfactant, increasing the temperature decreases the solubility of CH_4 in oil, but the reduction is relatively small, indicating that temperature has a minor influence on CH_4 solubility in n-decane. After the addition of surfactant ME-6, the solubility of CH_4 in n-decane is increased to some extent, with a noticeable enhancement in CH_4 solubility in n-decane at higher temperatures.

4.2.2. *Diffusion properties*

Fig. 18(a and b) investigates the diffusion characteristics of n-decane and CH_4 at 22.84 MPa with the addition of the surfactant ME-6, under different temperatures. The calculation involved determining the Mean Square Displacement (MSD) for both n-decane and CH_4. As depicted in Fig. 18(a and b), it can be observed that the diffusion rates of both n-decane and CH_4 increase with rising temperatures. This phenomenon is attributed to the elevation of molecular thermal energy with increasing temperature, resulting in greater kinetic energy. As n-decane molecules are in the liquid state, higher temperatures weaken the interactions among them, enabling freer diffusion and movement due to increased thermal energy. Consequently, the MSD increases as a consequence. CH_4 molecules, existing in a gaseous state, exhibit high dynamism influenced by thermal energy. As temperature rises, CH_4 molecules gain more kinetic energy, leading to enhanced speed and energy. The relatively weak interactions between CH_4 molecules facilitate their free propagation and diffusion within the system. This implies that CH_4 molecules cover a longer distance at the same time, subsequently increasing the MSD value. As a result, the MSD trend exhibits an upward trajectory with increasing temperature, reflecting the more active diffusion behavior of gas molecules at higher temperatures.

4.2.3. *Intermolecular forces*

To provide a microscale explanation for the effect of temperature on the reduction of interfacial tension (IFT) between CH_4 and n-decane in the presence of the surfactant ME-6, radial distribution functions (g(r)) are examined for different components before and

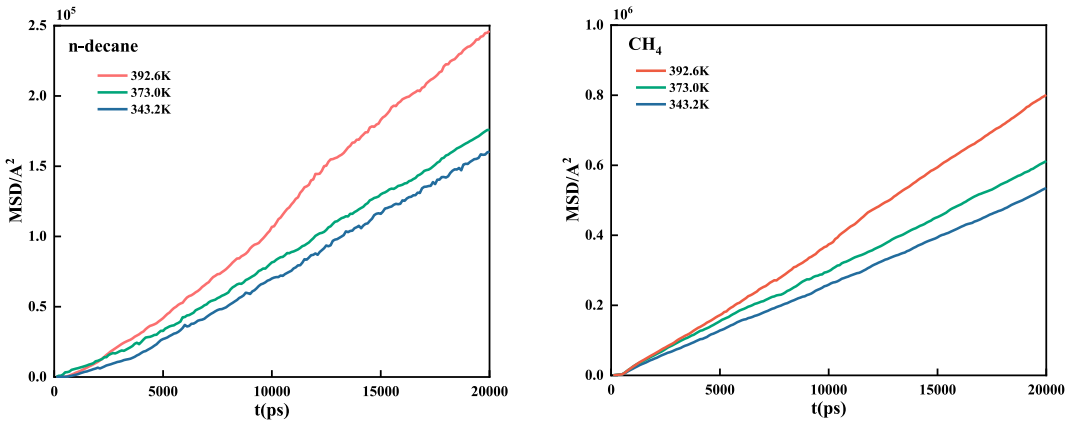

(a) MSD of n-decane (b) MSD of CH_4

Fig. 18. MSD of n-decane/CH_4 at different temperatures at 22.84 MPa.

after adding ME-6 under the same pressure but varying temperatures in the CH_4+n-decane system.

In the absence of the surfactant ME-6 (as illustrated in the left graphs of Fig. 19 (a) and (b)), elevated temperatures were found to decrease the g(r) peak values for n-decane-*n*-decane and n-decane-CH_4 interactions. This is predominantly due to the fact that interactions between n-decane molecules and between n-decane and CH_4 are primarily governed by van der Waals forces. As temperature increases, molecular thermal motion intensifies, leading to higher collision frequency between molecules. This results in enhanced repulsive components of van der Waals forces and weakened attractive components, causing an increase in molecular distances and subsequently diminishing the intermolecular forces.

Upon the introduction of the surfactant ME-6 into the system, as depicted in Fig. 19 (a) and (b) on the right, the peak of the radial distribution function (g(r)) between n-decane molecules decreases, while the peak of the g(r) between n-decane and CH_4 increases under the same temperature and pressure conditions. This phenomenon is attributed to the amphiphilic nature of the surfactant ME-6, leading to the formation of a molecular layer at the liquid interface.In the liquid phase, the hydrophobic end of the surfactant interacts with n-decane molecules, causing n-decane to accumulate at the oleophilic end of the surfactant layer. As a result, the intermolecular forces between n-decane molecules are reduced, leading to a decrease in their interaction forces, while the interaction forces between n-decane and CH_4 are enhanced.

At elevated temperatures, the intermolecular forces between n-decane molecules are augmented. This is due to the heightened molecular thermal motion at higher temperatures, causing the arrangement and orientation of surfactant molecules at the interface to change. This effect enhances the interaction between the oleophilic end of the surfactant and n-decane molecules, particularly as they approach each other more closely and form denser arrangements, thereby strengthening their interaction forces (as depicted in Figure 20a).

In the gas phase, as the temperature rises, CH_4 molecules exhibit more vigorous thermal motion, resulting in an increased repulsive component of the van der Waals forces. Thus, whether or not surfactant is added, the elevated temperature leads to an escalation in the repulsion between n-decane and CH_4 molecules, resulting in a reduction of their mutual interaction forces. The same trend applies to the interaction between CH_4 and the oleophobic end of the surfactant ME-6 (as shown in Fig. 20(b)).

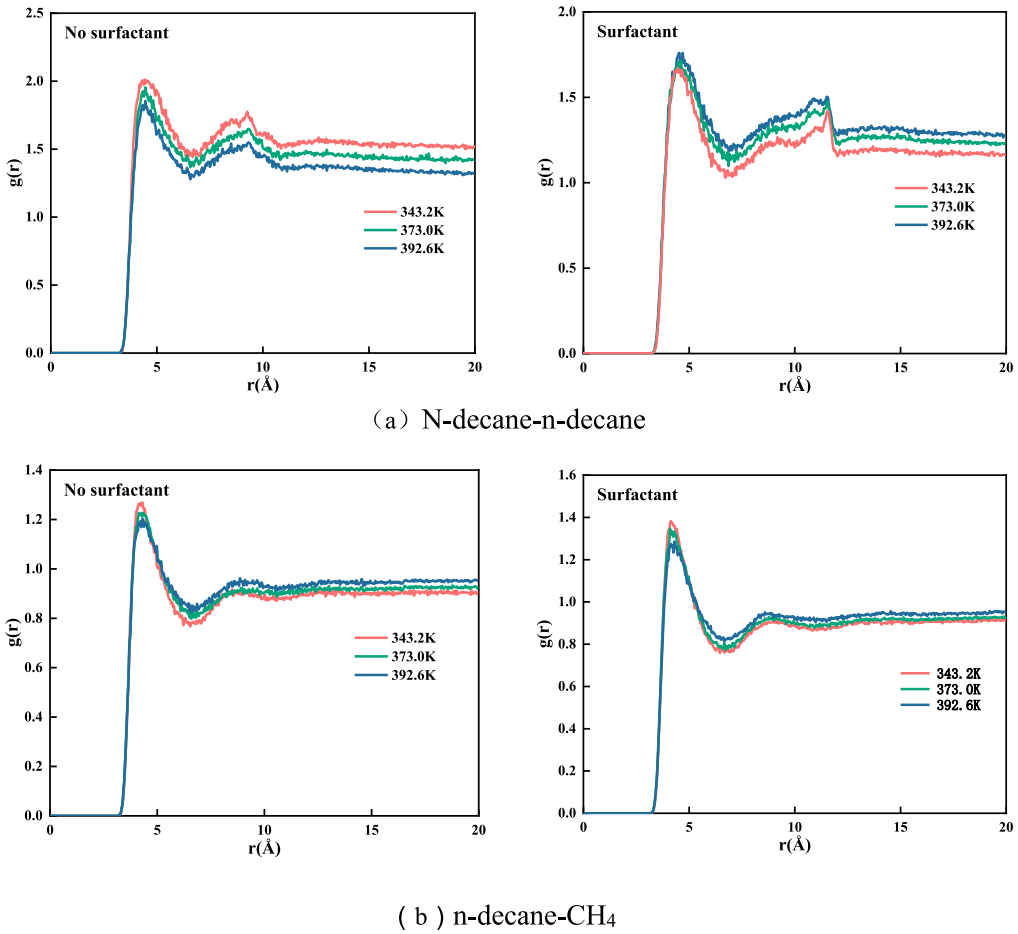

Fig. 19. Radial distribution function of n-decane/CH_4 in CH_4+ME-6+n-decane system at different temperatures (22.84 MPa).

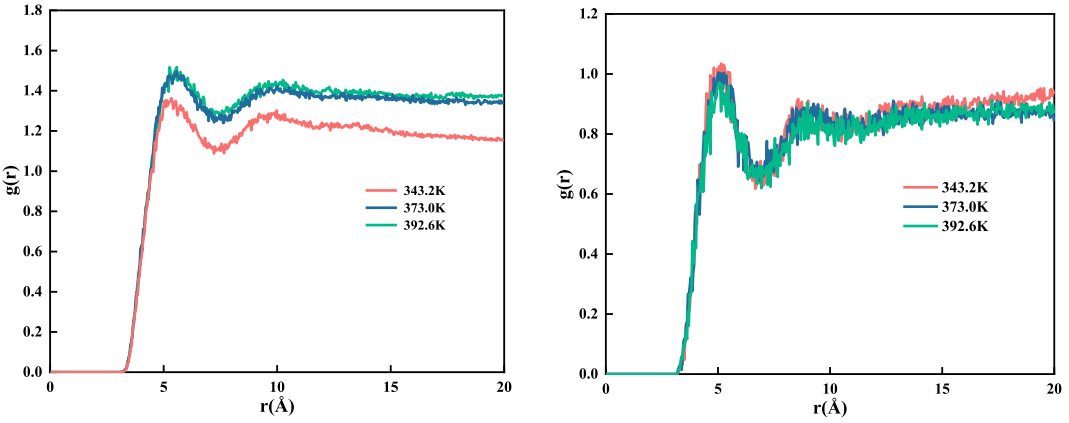

Fig. 20. Radial distribution functions (g(r)) between different components at various temperatures (22.84 MPa).

4.2.4. Interfacial tension and miscibility pressure

In general, temperature has a significant impact on the Minimum Miscibility Pressure (MMP) of CO_2-*n*-decane systems [46]. However, as observed from the data in Fig. 21 and Table 3, for the CH_4-*n*-decane system, the influence of temperature on MMP values is relatively small, even though there is still an increasing trend with rising temperature. This suggests that methane injection still favorable at higher temperatures. Moreover, at temperatures of 343.2 K, 373.0 K, and 392.6 K, the ME-6 surfactant shows a trend of reducing the Interfacial Tension (IFT) in the CH_4 + n-decane system. Among these, ME-6 demonstrates a better IFT reduction effect at 373.0 K compared to 343.2 K. Particularly, at 373.0 K, the interface tension reduction by ME-6 is more effective, with a decrease of 14.10% in MMP, while at 343.2 K, the decrease is 7.82%. This implies that ME-6 contributes to lowering the MMP under high-temperature reservoir conditions. The higher reduction in MMP could be attributed to the increased solubility of chemicals at higher temperatures, which enhances the miscibility between methane and n-decane. Therefore, the potential for further improving miscibility is relatively limited at lower temperatures. Based on the above analysis, the MMP values between methane and n-decane do not exhibit significant changes with an increase in temperature. Furthermore, under high-temperature conditions, the addition of a surfactant during methane injection provides the greater benefits.

5. Conclusions

In this study, we employed Molecular Dynamics (MD) simulations and the Vanishing Interfacial Tension (VIT) technique to investigate the effects of pressure and temperature on the equilibrium Interfacial Tension (IFT) of the CH_4+n-decane system. The goal was to explore the potential of chemically assisted methods to lower the Minimum Miscibility Pressure (MMP) in the CH_4+n-decane

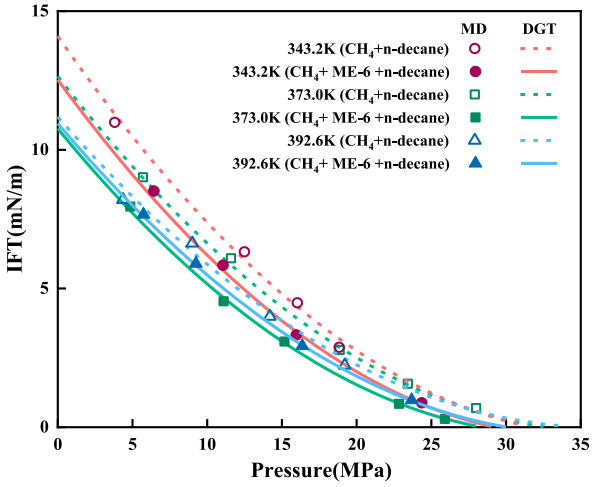

Fig. 21. Interfacial Tension (IFT) of CH_4 + ME-6 + n-decane system at different temperatures. The symbols represent the results from the MD simulations, and the estimates obtained using the DGT with VTPPR78 EoS are depicted as lines.

Table 3
MMP of CH_4 + ME-6 + n-decane system at different temperatures.

Temperature	MMP (MPa)	MMP reduction
343.2K	31.72	7.82%
	29.24	
373.0K	32.12	14.10%
	27.59	
392.6K	34.82	13.58%
	30.09	

system. We tested four different surfactants for their effectiveness in reducing MMP and identified the surfactant that achieved the best IFT reduction. Additionally, we conducted simulations to study the effect of this surfactant on MMP reduction in the CH_4+n-decane system at different temperatures. The results obtained are as follows:

1. The addition of surfactants can lower the IFT of the CH_4+n-decane system. Among them, the surfactant SOLOTERRA ME-6 exhibited the most effective reduction in MMP, showing a potential MMP decrease of 14.10% at 373 K.
2. Upon the addition of the surfactant ME-6 to the CH_4+n-decane system, an increase in pressure and temperature leads to a greater enrichment of CH_4 at the interface. This results in an enhanced solubility of CH_4 in n-decane.
3. After the addition of a surfactant, it was observed through the study of diffusion characteristics that CH_4 can more easily weaken the interactions between n-decane molecules, thereby enhancing the diffusion capacity of n-decane. Additionally, the interaction forces between CH_4 and n-decane are increased, facilitating the mixing of CH_4 and n-decane to achieve phase miscibility.
4. As the pressure increases, the peak of the interaction force between n-decane molecules and the oleophilic end of ME-6 gradually decreases, while the interaction force between CH_4 and the oleophobic end of ME-6 gradually increases. When the difference between these two forces decreases, the system approaches a mixed-phase state.
5. The MMP value between CH_4 and n-decane doesn't show significant changes with the increase in temperature. Under high-temperature conditions, the greatest benefits of adding the surfactant ME-6 during methane injection are observed.

Additional information

No additional information is available for this paper.

CRediT authorship contribution statement

Zhenzhen Dong: Conceptualization. **Shihao Qian:** Writing – original draft, Software, Methodology. **Weirong Li:** Writing – review & editing, Funding acquisition. **Xinle Ma:** Validation. **Tong Hou:** Investigation, Formal analysis. **Tianyang Zhang:** Validation, Formal analysis. **Zhanrong Yang:** Methodology. **Keze Lin:** Visualization. **Hongliang Yi:** Supervision, Data curation.

Declaration of competing interest

The authors declare that they have no known competing financial interests or personal relationships that could have appeared to influence the work reported in this paper.

Acknowledgements

Extensive appreciation is extended to the professors for their meticulous guidance in the selection, collection, and composition of this paper, to the laboratory colleagues for their vital technical assistance, and to the Graduate School of Xi'an Shiyou University for providing the research equipment and environment. This work was supported by PetroChina Innovation Foundation with Grant number 2022DQ02-0201.

References

[1] A.O. Gbadamosi, R. Junin, M.A. Manan, A. Agi, A.S. Yusuff, An overview of chemical enhanced oil recovery: recent advances and prospects, Int. Nano Lett. 9 (2019) 171–202, https://doi.org/10.1007/s40089-019-0272-8.
[2] M.S. Kamal, A.A. Adewunmi, A.S. Sultan, M.F. Al-Hamad, U. Mehmood, Recent advances in nanoparticles enhanced oil recovery: rheology, interfacial tension, oil recovery, and wettability alteration, J. Nanomater. 2017 (2017) 1–15, https://doi.org/10.1155/2017/2473175.
[3] M. Agista, K. Guo, Z. Yu, A state-of-the-art review of nanoparticles application in petroleum with a focus on enhanced oil recovery, Appl. Sci. 8 (2018) 871, https://doi.org/10.3390/app8060871.
[4] F.I. Stalkup, Status of miscible displacement, J. Petrol. Technol. 35 (1983) 815–826, https://doi.org/10.2118/9992-PA.
[5] H. Yu, Z. Yang, L. Luo, J. Liu, S. Cheng, X. Qu, et al., Application of cumulative-in-situ-injection-production technology to supplement hydrocarbon recovery among fractured tight oil reservoirs: a case study in Changqing Oilfield, China, Fuel 242 (2019) 804–818, https://doi.org/10.1016/j.fuel.2018.12.121.
[6] H. Yu, Z. Rui, Z. Chen, X. Lu, Z. Yang, J. Liu, et al., Feasibility study of improved unconventional reservoir performance with carbonated water and surfactant, Energy 182 (2019) 135–147, https://doi.org/10.1016/j.energy.2019.06.024.

[7] K. Zhang, N. Jia, F. Zeng, Application of predicted bubble-rising velocities for estimating the minimum miscibility pressures of the light crude oil–CO2 systems with the rising bubble apparatus, Fuel 220 (2018) 412–419, https://doi.org/10.1016/j.fuel.2018.01.100.
[8] H. Yu, X. Lu, W. Fu, Y. Wang, H. Xu, Q. Xie, et al., Determination of minimum near miscible pressure region during CO2 and associated gas injection for tight oil reservoir in Ordos Basin, China, Fuel 263 (2020) 116737, https://doi.org/10.1016/j.fuel.2019.116737.
[9] J.-C. Feng, Y. Wang, X.-S. Li, G. Li, Y. Zhang, Z.-Y. Chen, Effect of horizontal and vertical well patterns on methane hydrate dissociation behaviors in pilot-scale hydrate simulator, Appl. Energy 145 (2015) 69–79, https://doi.org/10.1016/j.apenergy.2015.01.137.
[10] Z. Yang, W. Wu, Z. Dong, M. Lin, S. Zhang, J. Zhang, Reducing the minimum miscibility pressure of CO2 and crude oil using alcohols, Colloids Surf. A Physicochem. Eng. Asp. 568 (2019) 105–112, https://doi.org/10.1016/j.colsurfa.2019.02.004.
[11] A. Al Adasani, B. Bai, Analysis of EOR projects and updated screening criteria, J. Petrol. Sci. Eng. 79 (2011) 10–24, https://doi.org/10.1016/j.petrol.2011.07.005.
[12] C.F. Kirby, M.A. McHugh, Phase behavior of polymers in supercritical fluid solvents, Chem. Rev. 99 (1999) 565–602, https://doi.org/10.1021/cr970046j.
[13] S.B. Hawthorne, D.J. Miller, C.B. Grabanski, L. Jin, Experimental determinations of minimum miscibility pressures using hydrocarbon gases and CO $_2$ for crude oils from the bakken and cut bank oil reservoirs, Energy Fuels 34 (2020) 6148–6157, https://doi.org/10.1021/acs.energyfuels.0c00570.
[14] Z. Dong, X. Ma, H. Xu, W. Li, S. Qian, Z. Wang, et al., Molecular dynamics study of interfacial properties for crude oil with pure and impure CH4, Appl. Sci. 12 (2022) 12239, https://doi.org/10.3390/app122312239.
[15] H. Luo, Y. Zhang, W. Fan, G. Nan, Z. Li, Effects of the non-ionic surfactant (C i PO j) on the interfacial tension behavior between CO 2 and crude oil, Energy Fuels 32 (2018) 6708–6712, https://doi.org/10.1021/acs.energyfuels.8b01082.
[16] P. Guo, Y. Hu, J. Qin, S. Li, S. Jiao, F. Chen, et al., Use of oil-soluble surfactant to reduce minimum miscibility pressure, Petrol. Sci. Technol. 35 (2017) 345–350, https://doi.org/10.1080/10916466.2016.1259630.
[17] C. Zhang, L. Xi, P. Wu, Z. Li, A novel system for reducing CO2-crude oil minimum miscibility pressure with CO2-soluble surfactants, Fuel 281 (2020) 118690, https://doi.org/10.1016/j.fuel.2020.118690.
[18] M. Almobarak, Z. Wu, M.B. Myers, C.D. Wood, N.S. Al Maskari, Y. Liu, et al., Chemical-assisted minimum miscibility pressure reduction between oil and methane, J. Petrol. Sci. Eng. 196 (2021) 108094, https://doi.org/10.1016/j.petrol.2020.108094.
[19] M. Almobarak, M.B. Myers, C.D. Wood, Y. Liu, A. Saeedi, Q. Xie, Oil systems: implications for natural gas injection to enhanced oil recovery, in: Chemical-assisted MMP Reduction on Methane-, Petroleum, 2022, https://doi.org/10.1016/j.petlm.2022.07.001.
[20] L. Jin, L.J. Pekot, S.B. Hawthorne, B. Gobran, A. Greeves, N.W. Bosshart, et al., Impact of CO2 impurity on MMP and oil recovery performance of the bell creek oil field, Energy Proc. 114 (2017) 6997–7008, https://doi.org/10.1016/j.egypro.2017.03.1841.
[21] S. Plimpton, Fast parallel algorithms for short-range molecular dynamics, J. Comput. Phys. 117 (1995) 1–19, https://doi.org/10.1006/jcph.1995.1039.
[22] S.K. Nath, F.A. Escobedo, J.J. de Pablo, On the simulation of vapor–liquid equilibria for alkanes, J. Chem. Phys. 108 (1998) 9905–9911, https://doi.org/10.1063/1.476429.
[23] M.G. Martin, J.I. Siepmann, Transferable potentials for phase equilibria. 1. United-atom description of n -alkanes, J. Phys. Chem. B 102 (1998) 2569–2577, https://doi.org/10.1021/jp972543+.
[24] W.L. Jorgensen, D.S. Maxwell, J. Tirado-Rives, Development and testing of the OPLS all-atom force field on conformational energetics and properties of organic liquids, J. Am. Chem. Soc. 118 (1996) 11225–11236, https://doi.org/10.1021/ja9621760.
[25] A. Stukowski, Visualization and analysis of atomistic simulation data with OVITO–the Open Visualization Tool, Model. Simulat. Mater. Sci. Eng. 18 (2010) 015012, https://doi.org/10.1088/0965-0393/18/1/015012.
[26] W.G. Hoover, A.J.C. Ladd, B. Moran, High-strain-rate plastic flow studied via nonequilibrium molecular dynamics, Phys. Rev. Lett. 48 (1982) 1818–1820, https://doi.org/10.1103/PhysRevLett.48.1818.
[27] S. Nosé, A unified formulation of the constant temperature molecular dynamics methods, J. Chem. Phys. 81 (1984) 511–519, https://doi.org/10.1063/1.447334.
[28] E.L. Pollock, J. Glosli, Comments on P3M, FMM, and the Ewald method for large periodic Coulombic systems, Comput. Phys. Commun. 95 (1996) 93–110, https://doi.org/10.1016/0010-4655(96)00043-4.
[29] F. Bresme, E. Chacón, P. Tarazona, Force-field dependence on the interfacial structure of oil–water interfaces, Mol. Phys. 108 (2010) 1887–1898, https://doi.org/10.1080/00268976.2010.496376.
[30] F. Bresme, E. Chacón, P. Tarazona, K. Tay, Intrinsic structure of hydrophobic surfaces: the oil-water interface, Phys. Rev. Lett. 101 (2008) 056102, https://doi.org/10.1103/PhysRevLett.101.056102.
[31] E.A. Müller, A. Mejía, Interfacial properties of selected binary mixtures containing n-alkanes, Fluid Phase Equil. 282 (2009) 68–81, https://doi.org/10.1016/j.fluid.2009.04.022.
[32] N. Choudhary, M.F. Anwari Che Ruslan, A.K. Narayanan Nair, R. Qiao, S. Sun, Bulk and interfacial properties of the decane + brine system in the presence of carbon dioxide, methane, and their mixture, Ind. Eng. Chem. Res. 60 (2021) 11525–11534, https://doi.org/10.1021/acs.iecr.1c01607.
[33] Y. Liang, S. Tsuji, J. Jia, T. Tsuji, T. Matsuoka, Modeling CO 2 –Water–Mineral wettability and mineralization for carbon geosequestration, Acc. Chem. Res. 50 (2017) 1530–1540, https://doi.org/10.1021/acs.accounts.7b00049.
[34] Y. Yang, A.K. Narayanan Nair, M.F. Anwari Che Ruslan, S. Sun, Bulk and interfacial properties of the decane + water system in the presence of methane, carbon dioxide, and their mixture, J. Phys. Chem. B 124 (2020) 9556–9569, https://doi.org/10.1021/acs.jpcb.0c05759.
[35] F.T. Smith, Atomic distortion and the combining rule for repulsive potentials, Phys Rev A 5 (1972) 1708–1713, https://doi.org/10.1103/PhysRevA.5.1708.
[36] Z. Mo, X. Zhu, G. Wang, W. Han, R. Guo, Molecular dynamics simulation on the interaction between single-walled carbon nanotubes and binaphthyl core-based chiral phenylene dendrimers, J. Mater. Res. 29 (2014) 2156–2161, https://doi.org/10.1557/jmr.2014.237.
[37] T.B. Stanishneva-Konovalova, O.S. Sokolova, Molecular dynamics simulations of negatively charged DPPC/DPPI lipid bilayers at two levels of resolution, Computational and Theoretical Chemistry 1058 (2015) 61–66, https://doi.org/10.1016/j.comptc.2014.04.036.
[38] D.N. Rao, J.I. Lee, Application of the new vanishing interfacial tension technique to evaluate miscibility conditions for the Terra Nova Offshore Project, J. Petrol. Sci. Eng. 35 (2002) 247–262, https://doi.org/10.1016/S0920-4105(02)00246-2.
[39] K. Zhang, Y. Gu, Two new quantitative technical criteria for determining the minimum miscibility pressures (MMPs) from the vanishing interfacial tension (VIT) technique, Fuel 184 (2016) 136–144, https://doi.org/10.1016/j.fuel.2016.06.128.
[40] M. Bayat, M. Lashkarbolooki, A.Z. Hezave, S. Ayatollahi, Investigation of gas injection flooding performance as enhanced oil recovery method, J. Nat. Gas Sci. Eng. 29 (2016) 37–45, https://doi.org/10.1016/j.jngse.2015.12.047.
[41] L.M.C. Pereira, A. Chapoy, R. Burgass, B. Tohidi, Measurement and modelling of high pressure density and interfacial tension of (gas + n -alkane) binary mixtures, J. Chem. Therm. 97 (2016) 55–69, https://doi.org/10.1016/j.jct.2015.12.036.
[42] J.-W. Qian, J.-N. Jaubert, R. Privat, Prediction of the phase behavior of alkene-containing binary systems with the PPR78 model, Fluid Phase Equil. 354 (2013) 212–235, https://doi.org/10.1016/j.fluid.2013.06.040.
[43] N. Choudhary, A.K. Narayanan Nair, Ruslan MFA. Che, S. Sun, Bulk and interfacial properties of decane in the presence of carbon dioxide, methane, and their mixture, Sci. Rep. 9 (2019) 19784, https://doi.org/10.1038/s41598-019-56378-y.
[44] M. Ghorbani, A. Momeni, S. Safavi, A. Gandomkar, Modified vanishing interfacial tension (VIT) test for CO2–oil minimum miscibility pressure (MMP) measurement, J. Nat. Gas Sci. Eng. 20 (2014) 92–98, https://doi.org/10.1016/j.jngse.2014.06.006.
[45] A. Trokhymchuk, J. Alejandre, Computer simulations of liquid/vapor interface in Lennard-Jones fluids: some questions and answers, J. Chem. Phys. 111 (1999) 8510–8523, https://doi.org/10.1063/1.480192.
[46] W.F. Yellig, R.S. Metcalfe, Determination and prediction of CO2 minimum miscibility pressures (includes associated paper 8876), J. Petrol. Technol. 32 (1980) 160–168, https://doi.org/10.2118/7477-PA.